Electronic Supplementary Material (ESI) for Physical Chemistry Chemical Physics.
This journal is © the Owner Societies 2014

Supporting Information

for

Clay-Supported Novel Bimetallic Core–Shell Co–Pt and Ni–Pt Nanocrystals with High Catalytic Activities

Dharmesh Varade[2,3] and Kazutoshi Haraguchi[1,2]*

1. Dep. of Applied Molecular Chemistry, College of Industrial Technology, Nihon University, 1-2-1 Izumi-cho, Narashino, Chiba 275-8575, Japan
2. Material Chemistry Laboratory, Kawamura Institute of Chemical Research, 631 Sakado, Sakura, Chiba 285-0078, Japan
3. Dep. of Chemical Engineering, Institute of Engineering & Technology, Ahmedabad University, Nr. Commerce Six Roads, Navrangpura, Ahmedabad-380 009, Gujarat, India

EXPERIMENTAL SECTION

Materials. An inorganic clay, synthetic hectorite (Laponite XLG $[Mg_{5.34}Li_{0.66}Si_8O_{20}(OH)_4]Na_{0.66}$), with a cation-exchange capacity of 104 mequiv/100 g (Rockwood, Ltd., UK) was used after being purified, washed, and vacuum-dried. Analytical grade potassium tetrachloroplatinate(II) (K_2PtCl_4), $NiCl_2$, $CoSO_4 \cdot 7H_2O$, 4-nitrophenol, and sodium borohydride ($NaBH_4$) were purchased from Wako Pure Chemical Industries, Ltd. (Japan). All of these reagents were used without further purification, unless

otherwise stated. Ultrapure water supplied by a PURIC-MX system (Organo Co., Japan) was used for all experiments.

Clay dispersion. Clay swells when dispersed in water and gradually cleaves into discrete disk-like particles of ~30 nm diameter and 1 nm thickness.[19] The clay particle shape is a result of the layered packing. A central sheet of O^{2-} and OH^{-} ions, defining octahedral sites that are occupied by Mg^{2+} ions, is sandwiched between two inverted sheets of tetrahedral silicates. The outer surfaces of these layers therefore comprise oxygen atoms that are involved in siloxane bonds. Hydroxyl groups are present on the edges of the particles. In synthetic Laponite XLG, the substitution of Li^{+} ions for 10% of the Mg^{2+} ions is the source of the negative charges. Dispersions of these inorganic particles were prepared by adding a known amount of powder to water with gentle mixing at 40 °C for 60 min. The resulting aqueous clay dispersion, which consisted of exfoliated clay particles, was homogeneous, transparent, and had a fairly high pH (10.2) and a negative zeta potential (–37.1 mV).[22]

Preparation of bimetallic nanocrystals. A typical synthesis of the bimetallic NCs is outlined below.

(1) For the Co–Pt NCs (Pt/Co molar ratio = 1.0), 10 mL K_2PtCl_4 solution (20 mM) and 10 mL $CoSO_4 \cdot 7H_2O$ solution (20 mM) were mixed with 10 mL clay dispersion (2 wt%) in a glass vial (50 mL).

(2) For the Ni–Pt NCs (Pt/Ni molar ratio = 1.0), 10 mL K_2PtCl_4 solution (20 mM) and 10 mL $NiCl_2$ solution (20 mM) were mixed with 10 mL clay dispersion (2 wt%) in a glass vial (50 mL).

Subsequently, 10 mL $NaBH_4$ solution (0.2 M) was quickly added to each vial [(1) and (2)] under sonication at room temperature. After sonication for 10 min, the mixture was left for

24 h at room temperature. The product was collected by centrifugation at 10,000 rpm for 10 min and then washed with water.

Catalytic reduction of 4-nitrophenol. A 0.5 mL sample of $NaBH_4$ solution (60 mmol/L) was added to 2.5 mL 4-nitrophenol solution (0.12 mmol/L) in a glass vessel. A known amount of catalyst was then added, and the mixture was stirred. Ultraviolet (UV) spectra of the samples were recorded immediately, and then at 60 s intervals, in the range 250–550 nm at 25 °C.

Characterization. The morphologies of the bimetallic NCs were examined using high-resolution field-emission transmission electron microscopy (TEM; JEM-2200TFE, JEOL) at 200 kV. The sample was prepared by depositing a drop of the dilute sample solution on a carbon-coated Cu grid and drying at room temperature. Energy-dispersive X-ray spectroscopy was performed using a scanning TEM detector fitted on a JEOL JEM-2200TFE instrument operated at 200 kV. X-ray photoelectron spectra were recorded using an ESCALab MKII X-ray photoelectron spectrometer fitted with a Mg Kα radiation excitation source. N_2 adsorption–desorption data were obtained using a BELSORP-mini II (BEL Japan Inc.) instrument operated at −196 °C. Prior to the measurements, the sample was added to the measurement cell, which was placed in a drying machine and heated at 80 °C overnight. After drying, helium gas was added to the cell. UV-visible (UV-vis) absorption spectra were recorded with samples in a quartz cuvette (1 mm) at room temperature, using a Hitachi U-4100 UV-vis double-beam spectrometer. Wide-angle powder X-ray diffraction patterns were obtained using a Rigaku SmartLab X-ray diffractometer with monochromated Cu Kα radiation (40 kV, 100 mA).

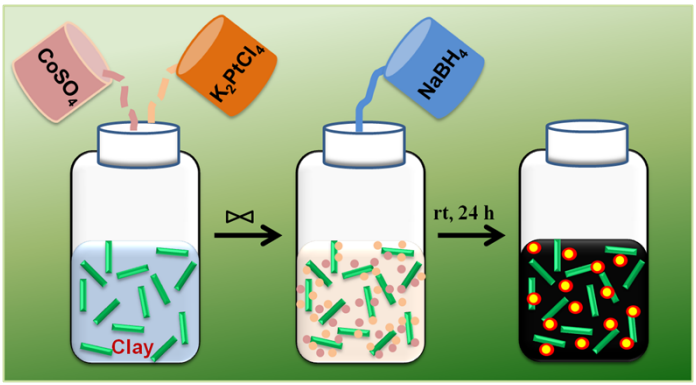

Scheme S1: Schematic representation of the preparation of the Co–Pt bimetallic NCs.

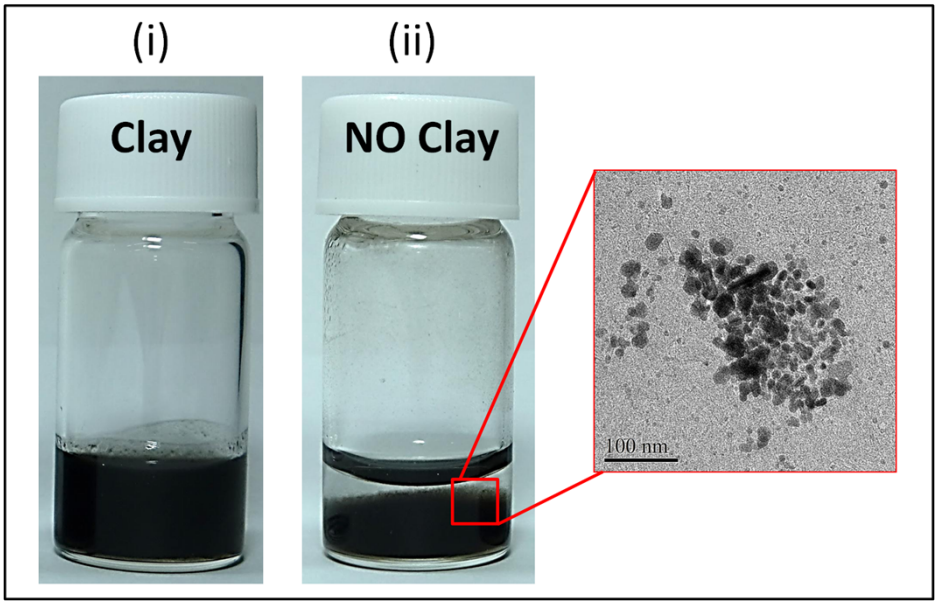

Figure S1: Optical images depicting the formation of an aqueous dispersion of Co–Pt bimetallic NCs prepared in the (i) presence and (ii) absence of clay. The inset shows the corresponding TEM image of the NCs in the absence of clay.

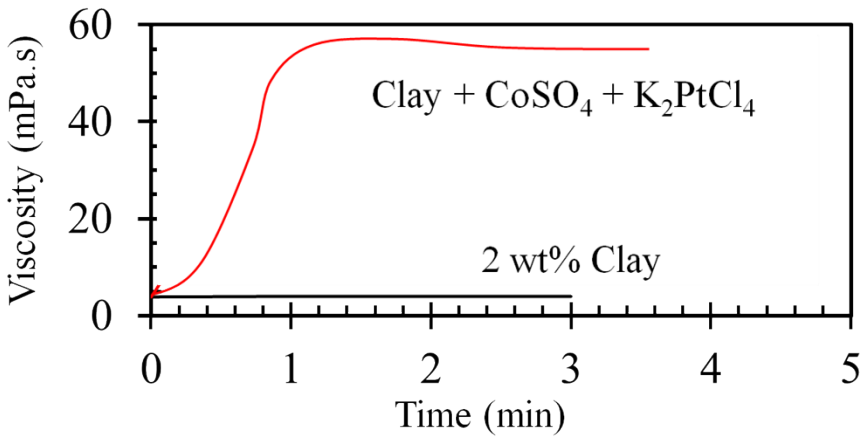

Figure S2: The viscosity change of a neat clay suspension (2 wt%) and a clay suspension (2 wt%) upon addition of K_2PtCl_4 (20 mM) and $CoSO_4$ (20 mM).

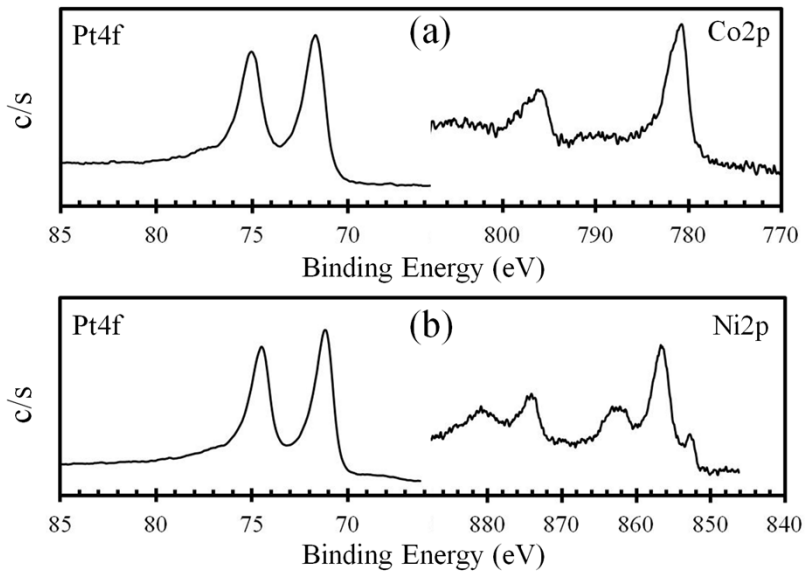

Figure S3: X-ray photoelectron spectra (XPS) for (a) Co–Pt and (b) Ni–Pt core–shell NCs.

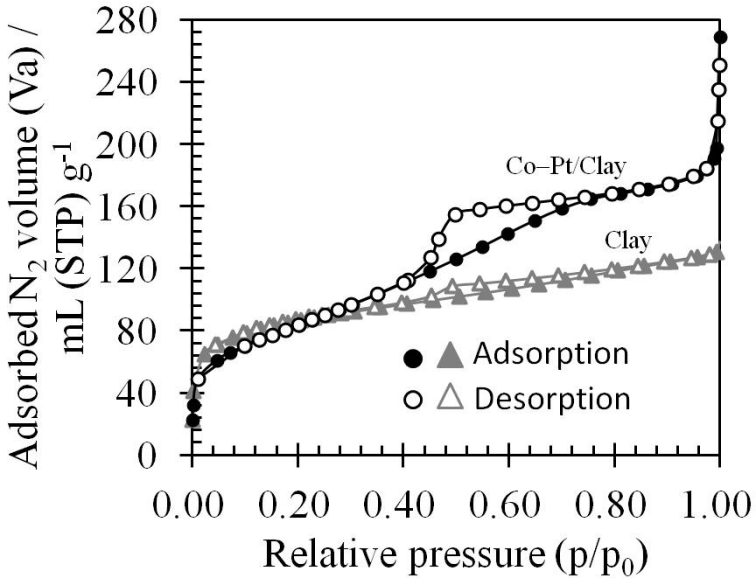

Core–Shell NC/Clay	Surface Area a_s (BET) ($m^2 g^{-1}$)	Average Pore Size (nm)	Pore Volume ($cm^3 g^{-1}$)
Clay	314	4.04	0.10
Co–Pt/clay	240	4.51	0.14

Figure S4: N_2 adsorption–desorption measurements for the clay and the Co–Pt/clay composites. The table illustrates the data analysis for the N_2 adsorption–desorption measurements.

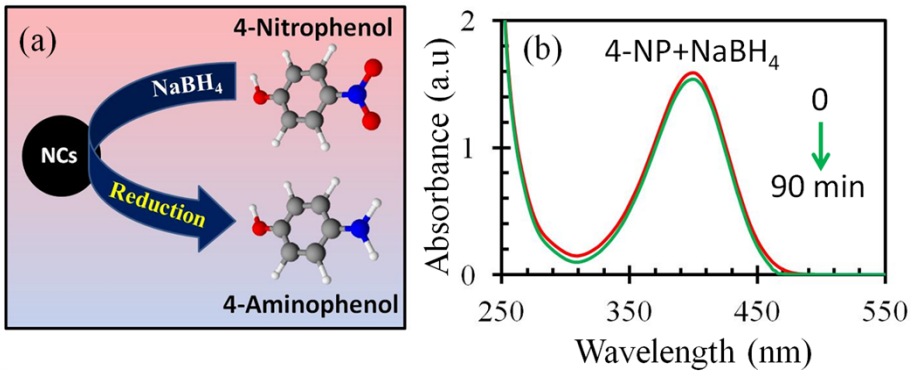

Figure S5: (a) The catalytic activities of the Co–Pt and Ni–Pt core–shell NCs were tested for the reduction of 4-nitrophenol with $NaBH_4$ as a model system. (b) Ultraviolet-visible (UV-vis) spectra of 4-nitrophenol (4-NP) and 4-NP + $NaBH_4$. There was no change in the UV-vis spectrum after 90 min in the absence of catalyst.

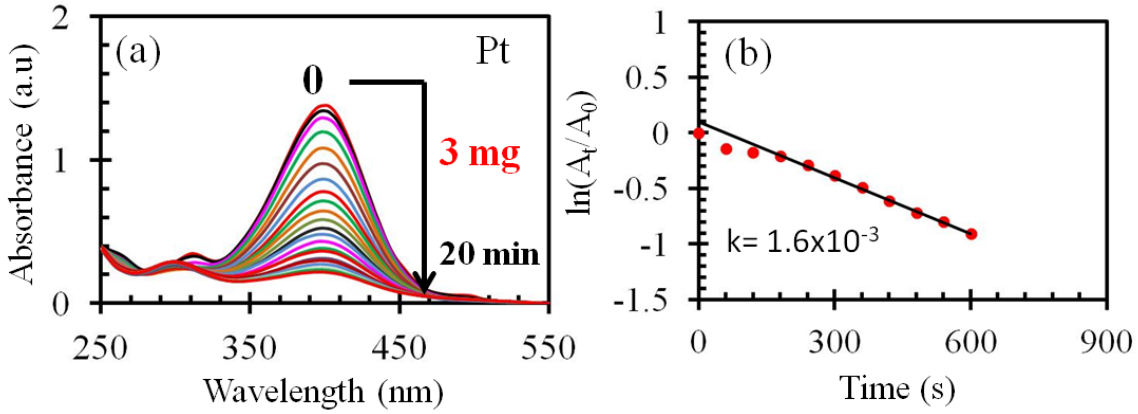

Figure S6: (a) Temporal evolution of the UV-vis spectra for the reduction of 4-nitrophenol by $NaBH_4$ in the presence of monometallic Pt NCs. (b) Linear correlation of $\ln(A_t/A_0)$ with time (A_t and A_0 represent the absorbance at time t and the initial absorbance of 4-nitrophenolate ions, respectively) for as-prepared Pt NCs. The black lines show the slopes, which correspond to the rate constants (k).

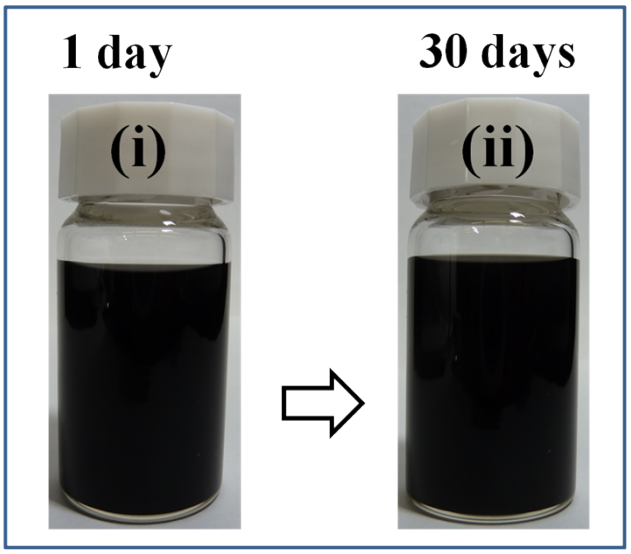

Figure S7: Optical images depicting the stability of the aqueous dispersion of Co–Pt bimetallic NCs (i) 1 d and (ii) 30 d after its initial preparation.